

Article

Mechanism of Free Silver Formation While Preparing Silver-Coated Copper Powder by Chemical Plating and Its Control

Junquan Chen ¹, Xiaoyun Zhu ^{1,*} , Nan Yang ¹, Xiang Li ^{2,*} and Bingzhe Yang ¹

¹ School of Materials Science and Engineering, Kunming University of Science and Technology, Kunming 650031, China; c2298405268@163.com (J.C.); yn009612819@163.com (N.Y.); yang_5413@163.com (B.Y.)

² Yunnan Spring New Material Co., Ltd., Kunming 650212, China

* Correspondence: xyzhu@kust.edu.cn (X.Z.); li39198790@163.com (X.L.)

Abstract: When silver-coated copper powder is produced through chemical plating, free silver is often formed, which not only lowers coating quality but also increases the consumption of silver salt. Therefore, understanding the mechanism of free silver formation during the chemical plating process is essential for improving this process and enhancing the quality of silver-coated copper powder. This paper investigates the contents of free silver as well as the morphology and properties of the powder under different conditions by varying reaction parameters during the preparation of silver-coated copper powder. The morphology, phase, and properties of the powder samples are characterized using scanning electron microscopy (SEM), X-ray diffraction (XRD), and a resistance tester. In addition, the cathodic polarization behavior of the plating solution is analyzed using an electrochemical workstation. The results show that the complexing agent, reaction temperature, main salt drop acceleration rate, and dispersant concentration all affect the generation of free silver, and the complexing agent has the greatest impact.

Keywords: chemical plating; free silver; complexing agent; drop acceleration rate; dispersant concentration



Academic Editor: Alessandro Patelli

Received: 10 January 2025

Revised: 26 January 2025

Accepted: 1 February 2025

Published: 3 February 2025

Citation: Chen, J.; Zhu, X.; Yang, N.; Li, X.; Yang, B. Mechanism of Free Silver Formation While Preparing Silver-Coated Copper Powder by Chemical Plating and Its Control. *Coatings* **2025**, *15*, 169. <https://doi.org/10.3390/coatings15020169>

Copyright: © 2025 by the authors. Licensee MDPI, Basel, Switzerland. This article is an open access article distributed under the terms and conditions of the Creative Commons Attribution (CC BY) license (<https://creativecommons.org/licenses/by/4.0/>).

1. Introduction

Among commonly used conductive phases, copper is favored for its ease of processing and excellent electrical properties. However, the stability of metallic copper is a concern, as it is prone to oxidation in air, forming copper oxide, which reduces its conductivity [1–3]. Furthermore, conductive phases used in most conductive pastes are ultrafine powders at the micron and nanometer scale. At these sizes, the activation energy of the metal surface is high, making metallic copper more susceptible to oxidation. Therefore, ultrafine copper powder is not suitable for direct use as a conductive filler in conductive paste. Silver-coated copper powder, on the other hand, consists of a copper core coated with a layer of silver. It combines the excellent thermal and oxidation stability of silver with the low cost of copper [4,5]. Therefore, developing a method to prepare high-performance silver-coated copper powder has become a key technology for reducing the cost of conductive pastes.

Currently, silver plating methods include vapor deposition [6,7], mechanical grinding, and chemical plating [8–12]. Vapor deposition requires special equipment and complex processes, while mechanical grinding consumes more silver during the preparation of silver-coated copper powder. Chemical plating, on the other hand, has a simple process

and low equipment requirements. However, the reaction for chemical plating is carried out in solution, and the stability of the plating system is relatively poor. The chemical plating process is mainly divided into water-soluble and organic solvent systems. Due to the high cost associated with the organic solvent system, it is not suitable for large-scale silver plating [13,14].

In previous studies, it was found that the use of ethylenediaminetetraacetic acid can control the rate at which silver is reduced. If the complexing agent is insufficient, the rate of silver reduction by hydrazine is very fast even at very low reactant concentrations and temperatures [15]. The silver-coated copper powder can be successfully prepared using glucose as a reducing agent and ammonia as a complexing agent. However, the $[\text{Cu}(\text{NH}_3)_4]^{2+}$ generated by the side reaction during the reaction adheres to the surface of the copper powder matrix. Adding an appropriate amount of ethylenediamine can avoid the generation and adsorption of $[\text{Cu}(\text{NH}_3)_4]^{2+}$, ensuring the integrity and density of the silver layer coating [16]. The concentration of the dispersant will affect the structure and size of the prepared nanomaterials. When preparing silver nanomaterials, polyvinylpyrrolidone (PVP) and the (100) crystal plane of Ag are more likely to form an encapsulation structure. By changing the concentration and molecular weight of PVP in the solution, the surface coverage can be changed, and the morphology of Ag nanocubes can be changed [17,18]. This paper mainly studies the generation of free silver in chemical silver plating, analyzes the various experimental factors in chemical plating and the effects on the generation of free silver, analyzes the causes of free silver generation, and how to improve silver deposition.

2. Materials and Methods

2.1. Experimental Materials

Table 1 shows the properties of the copper powder raw materials. Sodium hydroxide, sulfuric acid, polyvinyl pyrrolidone (PVP), silver nitrate, glucose, ascorbic acid, hydrazine hydrate, ammonia water, ethylenediamine, and triethylenetetramine are all analytically pure.

Table 1. Copper powder parameters.

Powder Parameters	
Copper powder shape	Spherical
Average particle size	3.5 μm
Specific surface area	0.34~0.42 m^2/g
Tap density	$\geq 4.5 \text{ g}/\text{cm}^3$

2.2. Experimental Procedures

2.2.1. Copper Powder Pretreatment

1. Weigh 10 g of copper powder and transfer it into a beaker. Add 300 mL of a 3 g/L sodium hydroxide solution, and then sonicate for 10 min to remove the protective agent from the surface of the copper powder.
2. Wash the copper powder twice with deionized water.
3. Add 300 mL of 1 g/L sulfuric acid solution and perform ultrasonic treatment for 10 min to remove the oxides of the copper powder.
4. Rinse the copper powder with deionized water until the pH of the supernatant reaches 7.

2.2.2. Chemical Silver Plating

5. Add an appropriate amount of deionized water and polyvinyl pyrrolidone to the treated copper powder to prepare a copper powder suspension.

6. Do mechanical stirring and ultrasonic dispersion for 20 min.
7. Add the silver complex solution and the reducing agent solution to the dispersed copper powder suspension. Allow the reaction to proceed until completion.
8. After the reaction is completed, the silver-coated copper powder is washed twice with deionized water, centrifuged, and dried to obtain the final product.

2.3. Property Testing and Characterization

The surface morphology and particle size of the silver-coated copper powder were observed by a JSM-7800F field emission scanning electron microscope (SEM) (JEOL, Tokyo, Japan). The sheet resistance of the silver-coated copper powder was tested by a TH2512 resistance tester (Changzhou Tonghui Electronics Co., Ltd., Changzhou, China). The phase analysis of the silver-coated copper powder was performed by a TD-3500 X-ray diffraction analysis (XRD) (Dandong Tongda Technology Co., Ltd., Dandong, China). The cathodic polarization curve of the silver complex solution was tested by a DH7006 electrochemical workstation (Shanghai Chenhua Instrument Co., Ltd., Shanghai, China). The working electrode was a square silver-plated copper sheet with a side length of 1 cm, the auxiliary electrode was a platinum electrode, the reference electrode was a silver electrode, and the potentiodynamic scanning speed was 1 mV/s.

3. Results and Discussion

3.1. Effects of Complexing Agents and Reducing Agents on Formation of Free Silver

Silver ions can react with various complexing agents to form silver complexes in solution. In this experiment, ammonia ($\text{NH}_3 \cdot \text{H}_2\text{O}$), ethylenediamine (EDA), and triethylenetetramine (TETA) are selected as complexing agents to form silver complexes with silver nitrate. Glucose, ascorbic acid, and hydrazine hydrate are used as reducing agents to reduce the respective silver complexes. To investigate the effects of different reducing agents and silver complexes on the formation of free silver during chemical plating, nine experimental groups are designed, as shown in Table 2. In each group, different complexing agents are first used to form silver complexes with silver ions, followed by using various reducing agents to reduce the silver complex ions.

Table 2. Complexing agents and reducing agents used in chemical plating.

Serial Number	Reducing Agent	Complexing Agent
1#	Glucose	Ammonia
2#	Glucose	Ethylenediamine
3#	Glucose	Triethylenetetramine
4#	Ascorbic acid	Ammonia
5#	Ascorbic acid	Ethylenediamine
6#	Ascorbic acid	Triethylenetetramine
7#	Hydrazine hydrate	Ammonia
8#	Hydrazine hydrate	Ethylenediamine
9#	Hydrazine hydrate	Triethylenetetramine

Figure 1 presents SEM images of the silver-coated copper powder prepared using the respective complexing and reducing agents listed in Table 2. As observed in Figure 1, samples 1#, 4#, and 7# contain a large amount of free silver, while the free silver content in samples 2#, 5#, and 8# is significantly lower. In contrast, samples 3#, 6#, and 9# show almost no free silver. A common feature of the three sets of samples is that the complexing agent is the same, while the reducing agent varies. This suggests that the complexing agent plays a more significant role in controlling the formation of free silver during the chemical plating process than the reducing agent.

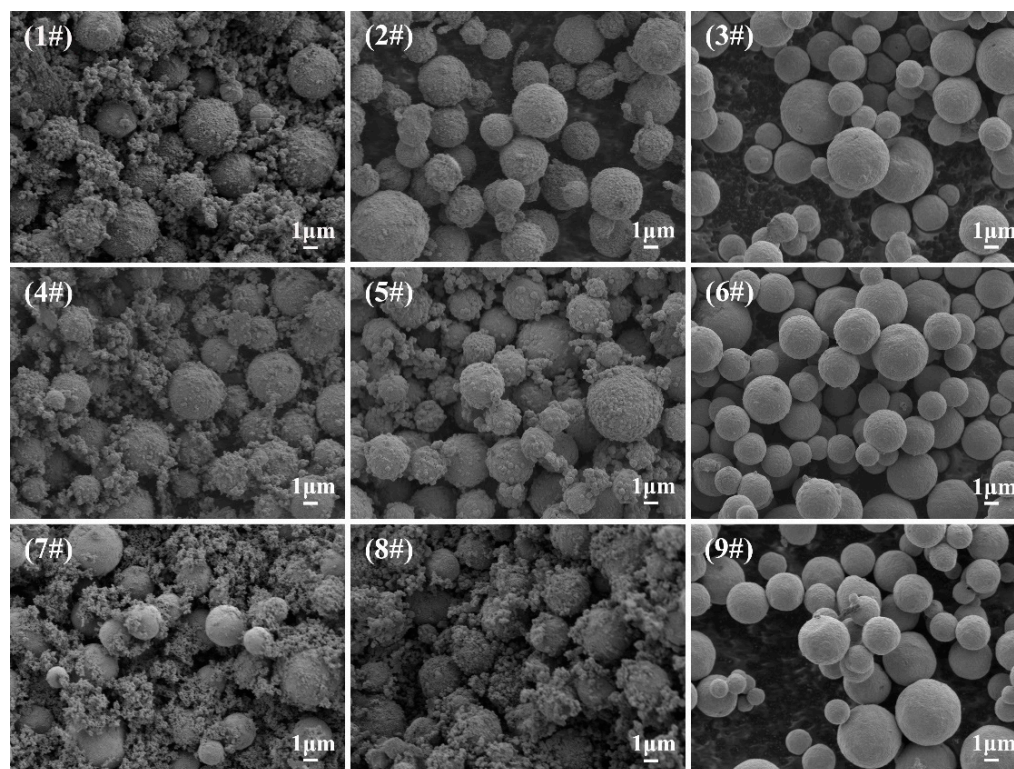


Figure 1. SEM images of silver-coated copper powder prepared with different complexing agents and reducing agents.

In the silver complex solution, the stability of different silver complex ions can be characterized by cathode polarization. Figure 2 shows cathode polarization curves of the working electrode in the silver complex solution with ammonia ($\text{NH}_3 \cdot \text{H}_2\text{O}$), ethylenediamine (EDA), and triethylenetetramine (TETA) as complexing agents. As shown in the figure, in the initial potential range ($0 \sim -0.0625 \text{ V}$), the current density is low, and the silver complex ions are not deposited at the cathode. As the electrode potential becomes negative ($-0.0625 \sim -0.25 \text{ V}$), the current density begins to rise. Once the electrode potential drops below -0.25 V , the polarization curves start to show differences. Among them, the slope of the polarization curve of the silver complex solution with triethylenetetramine (TETA) as the complexing agent is the smallest, the current density rises the slowest, and the cathode polarization of the silver complex solution is the most extensive, indicating that the silver complex formed by triethylenetetramine (TETA) and silver ions is most stable.

Figure 3 presents the Tafel curves of three silver complex solutions. A smaller slope indicates faster charge transfer during the reaction process of the electrode in the solution system. As illustrated in Figure 3, the silver complex solution with ammonia water as the complexing agent exhibits the smallest Tafel curve slope, indicating the fastest charge transfer and, consequently, the fastest reaction rate. In contrast, the Tafel curve of the silver complex solution with triethylenetetramine (TETA) as the complexing agent has the largest slope, suggesting the slowest charge transfer rate and hence the slowest reaction rate. Summarizing the analysis of Figures 2 and 3, it can be concluded that the silver complex solution using triethylenetetramine as the complexing agent is stable and exhibits the slowest reaction rate. During the chemical plating process, the silver complex solution with triethylenetetramine not only shows good stability but also significantly reduces the silver reduction rate. This results in a marked reduction in the amount of free silver in the prepared silver-coated copper powder. This aligns with the observations in Figure 1,

that is, silver-coated copper powders corresponding to 3#, 6#, and 9#, prepared using triethylenetetramine as the complexing agent, contain the least amount of free silver.

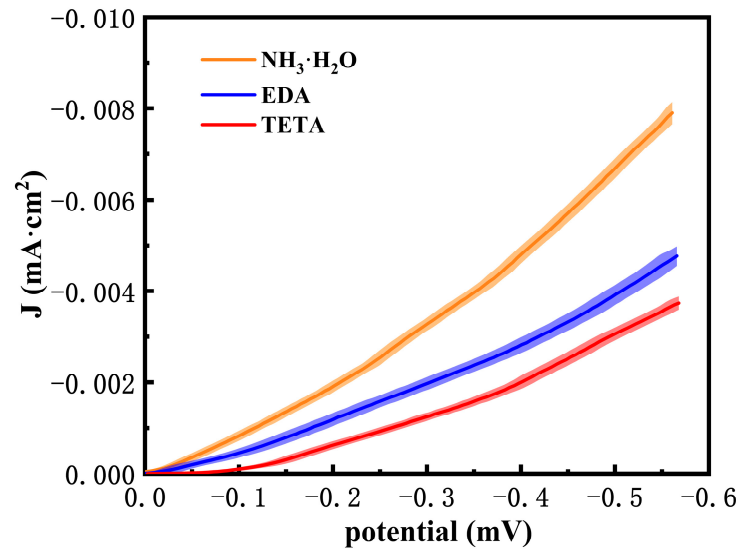


Figure 2. LSV curve of the silver complex solution.

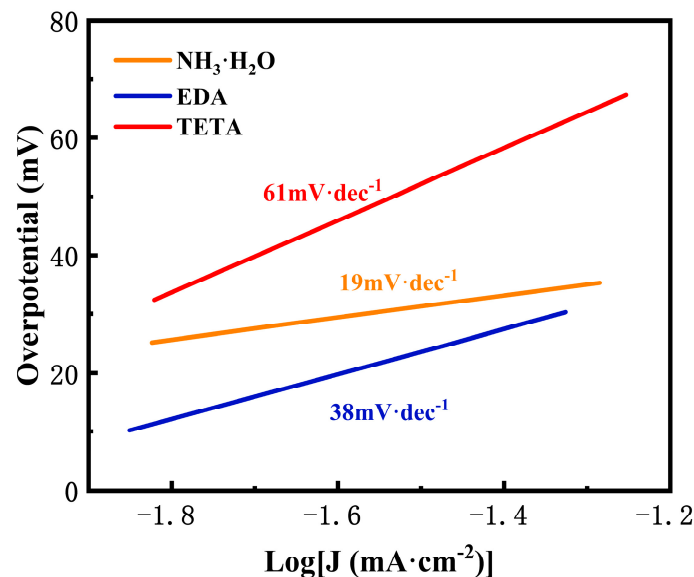


Figure 3. Tafel plots of different silver complex solutions.

The Tafel curve illustrates the effect of ammonia, ethylenediamine, and triethylenetetramine on the reaction rate during chemical silver plating. From this curve, it is evident that the stronger the complexing ability of the complexing agent with silver, the greater the impact on the reaction rate. Using a complexing agent with a strong affinity for silver significantly reduces the reaction rate, which in turn leads to a considerable reduction in the amount of free silver in the resulting silver-coated copper powder.

On the other hand, a substitution reaction occurs during the chemical plating process. Ag^+ ions can form silver complexes with various complexing agents in the solution, which reduces the concentration of free Ag^+ . Additionally, since the complexing agents have a higher molecular weight than Ag^+ , and the diffusion coefficient of the resulting silver complex ions is lower than that of free Ag^+ , the rate of the substitution reaction is significantly reduced. This reduction in reaction rate limits the formation and growth rate of silver nuclei, allowing the silver nuclei to deposit more effectively on the surface of copper powder, thereby reducing the formation of free silver [19–22].

While selecting a reducing agent for silver plating, the type of complexing agent must also be considered. When a strong reducing agent is combined with a less stable complexing agent, Ag^+ is more likely to be directly reduced to elemental silver particles. When ammonia and ethylenediamine are used as complexing agents and hydrazine hydrate is used as a reducing agent, the prepared silver-coated copper powder contains a large amount of free silver, while using glucose as a reducing agent can reduce the generation of free silver. Conversely, when a weak reducing agent is paired with a more stable complexing agent, the silver plating reaction may take longer, reducing the overall preparation efficiency. When triethylenetetramine is used as a complexing agent, using glucose as a reducing agent will increase the reaction time, while using ascorbic acid as a reducing agent can both control the generation of free silver and ensure the efficiency of the experiment. Additionally, some reducing agents exhibit varying reducibility under different conditions. For example, the reducibility of ascorbic acid and glucose changes with pH. Therefore, when choosing a reducing agent, it is crucial to account for the influence of reaction conditions on its reducibility. For experiments that follow in this study, ascorbic acid is used as the reducing agent, and triethylenetetramine as the complexing agent to prepare silver-coated copper powder, with a focus on how experimental parameters affect the formation of free silver.

3.2. Effect of Temperature on Free Silver

Figure 4 presents SEM images of the silver-coated copper powders obtained at these different temperatures. As demonstrated, at 30 °C, the low reaction rate leads to a reduced nucleation rate of silver on the surface of the copper powder. While crystal nuclei can form and grow, the silver deposition is concentrated in areas with existing nuclei, resulting in silver adhering to the copper powder surface in the form of large particles [23]. Since the reaction occurs under stirring conditions, the protruding silver particles are prone to falling off due to collisions with other powder particles, forming free silver. Consequently, the powder prepared at this temperature exhibits a high content of free silver.

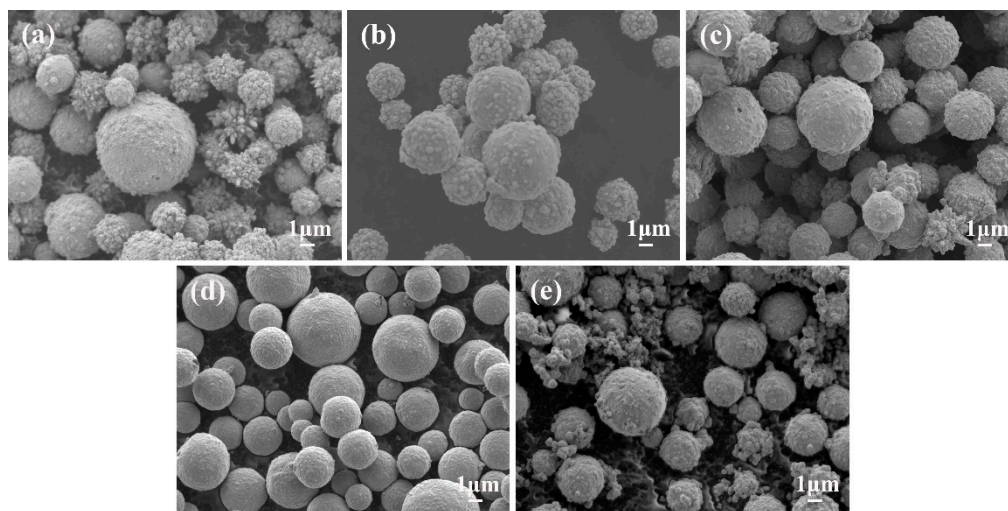


Figure 4. SEM images of silver-coated copper powder prepared at different reaction temperatures: (a) 30 °C, (b) 35 °C, (c) 40 °C, (d) 45 °C, and (e) 50 °C.

With an increase in temperature, the rate of silver reduction gets higher, leading to a higher nucleation rate of silver on the copper powder surface [24,25]. This results in a more uniform silver layer growth, preventing the formation of large silver particles on the surface of the powder. The surface of the powder becomes flatter and smoother, and the silver deposited on the copper powder is more securely adhered, making it less likely to be

dislodged by collisions during the reaction. Consequently, the content of free silver in the prepared silver-coated copper powder decreases.

At 50 °C, the silver particles move faster. As a result, when silver particles collide with the copper powder surface, the time they spend on the surface is reduced due to their increased speed, which does not help with their deposition. Additionally, some silver particles may not deposit to the copper powder surface but instead grow independently after colliding and contacting each other. Alternatively, silver particles already adhered to the copper powder surface may be dislodged by collisions with other particles, forming free and dispersed silver particles. This leads to a higher content of free silver in the powder.

Figure 5 presents the XRD patterns of silver-coated copper powders prepared. The characteristic peaks of metallic silver (Ag) appear at $2\theta = 38.2^\circ$, 44.2° , 64.6° , and 77.4° , corresponding to the (111), (200), (220), and (311) crystal planes, respectively. The characteristic peaks of metallic copper (Cu) are observed at $2\theta = 43.3^\circ$, 50.5° , and 74.1° , corresponding to the (111), (200), and (220) crystal planes, respectively. The results indicated that the prepared powder was composed solely of silver and copper, without any detectable impurities.

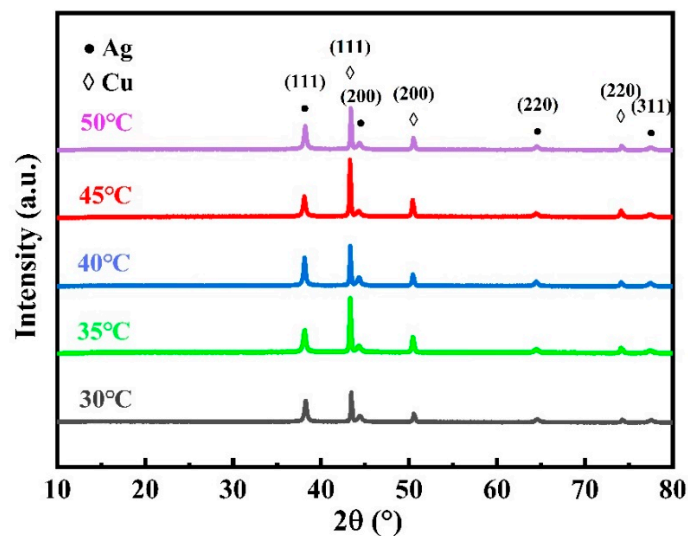


Figure 5. XRD pattern of silver-coated copper powder.

Figure 6 presents the relationship between temperature, the half-peak width of silver, and the crystal size. Full width at half maximum (FWHM) refers to a measure of the width of the diffraction peak in the X-ray diffraction (XRD) spectrum. It represents the half-height width of the diffraction peak, that is, the width of the peak when the intensity of the diffraction peak reaches half of the maximum value. The size of the half-width can reflect information such as the size and crystallinity of the grains in the sample. There is a certain inverse relationship between the half-width and the grain size [26]. According to the Scherrer equation, the grain size is calculated by the half-width of the diffraction peak. The formula for Scherrer's law is as follows:

$$D = \frac{K\lambda}{\beta \cos\theta} \quad (1)$$

where

D is the average size of the grains;

K is the shape factor;

λ is the wavelength of the X-ray;

β is the half-peak width (in radians);

θ is the diffraction angle.

From this formula, it can be seen that the half-peak width β is inversely proportional to the grain size D , that is, the larger the half-peak width, the smaller the grain size, and vice versa. As shown, as the temperature increases, the half-peak width of silver broadens, while the crystal size reduces. This indicates that in the preparation process of chemically silver-plated copper powder, temperature will affect the half-peak width and crystal size of silver, thereby affecting the deposition and growth of silver on the surface of copper powder. Notably, at 45 °C, the half-peak width of silver is at maximum, and the crystal size is at minimum.

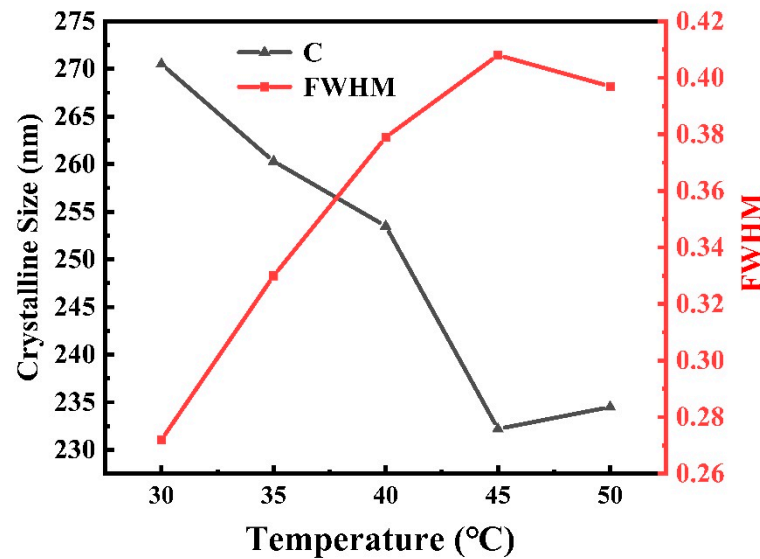


Figure 6. Half-peak width and crystal size of silver at different temperatures.

Figure 7 shows the sheet resistance curves of silver-coated copper powder prepared at different temperatures. Silver and copper have different crystal structures and conductive properties. Ideally, silver should be evenly coated on the surface of copper particles, but too much free silver may cause the silver layer to become uneven or even have areas where the silver layer is weak. In these areas, the copper surface may be exposed, and although the conductivity of copper is high, it is much lower than that of silver. Therefore, the conductivity of silver-coated copper powder will be significantly affected. If there is too much free silver, the silver layer will not be fully covered, which may reduce the conductivity. Too much free silver may have a negative impact on the overall structural stability of the powder, causing powder aggregation or loose structure. Structural instability may make the conductive path uneven, which in turn leads to a decrease in conductivity. Coatings or powders with a tight and uniform structure usually have better conductivity, and too much free silver may break this structural stability. As shown in Figure 7, the resistance decreases with increasing temperature. By correlating this with the data in Figure 4, it can be observed that at 30 °C, the free silver content in the silver-coated copper powder is relatively high, indicating that there are more free silver particles, which affects the conductivity of the powder. The conductivity is best at 45 °C, corresponding to the lowest free silver content.

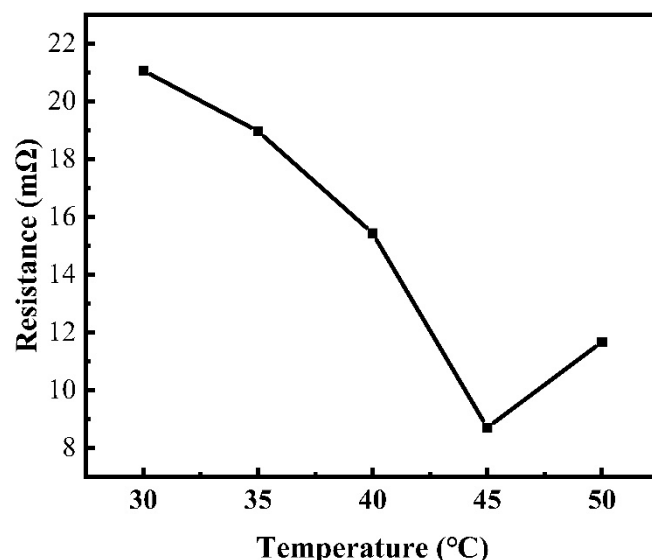


Figure 7. Sheet resistance for silver-coated copper powder made at different temperatures.

3.3. Effect of Main Salt Addition Rate on the Formation of Free Silver

During the preparation of silver-coated copper powder via chemical plating, the rate at which the main salt is added not only affects the concentration of silver ions in the reaction system but also the pH of the system. Since the silver complex solution used in this experiment is alkaline, different addition rates can cause significant changes in the pH value. The pH of the silver amine solution is 11. To examine the effect of the main salt addition rate on the formation of free silver, the dropping rate of ascorbic acid is kept constant at 8–10 mL/min. The silver complex solution is introduced into the copper powder suspension at three different rates: 3–5 mL/min, 8–10 mL/min, and 13–15 mL/min. Silver-coated copper powders are prepared at these varying addition rates, and their morphology is observed using scanning electron microscopy.

Figure 8 presents the SEM image of silver-coated copper powder obtained at different main salt addition rates, while Figure 9 illustrates the silver plating model at these rates. As seen in Figure 8, when the main salt addition rate is 3–5 mL/min, a larger amount of silver particles is deposited on the powder surface, with the deposited particles being relatively larger in size. This results in an uneven surface and reduced flatness of the powder. Also, there is an increase in the amount of free silver in the powder. The presence of free silver leads to reduced silver coverage in the copper powder, which negatively affects the quality of the silver-coated copper powder.

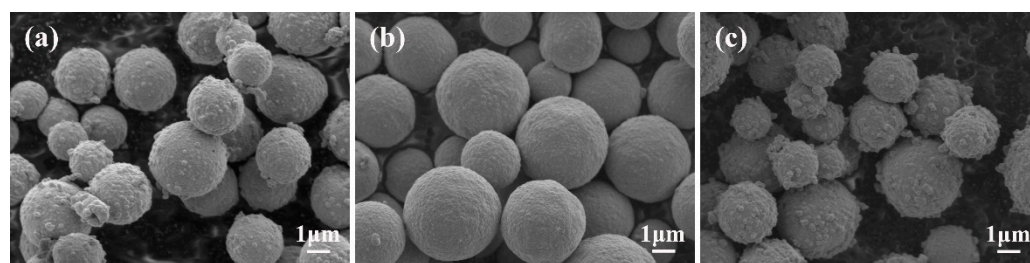


Figure 8. SEM images of silver-coated copper powder obtained at different main salt addition rates: (a) 3–5 mL/min, (b) 8–10 mL/min, and (c) 13–15 mL/min.

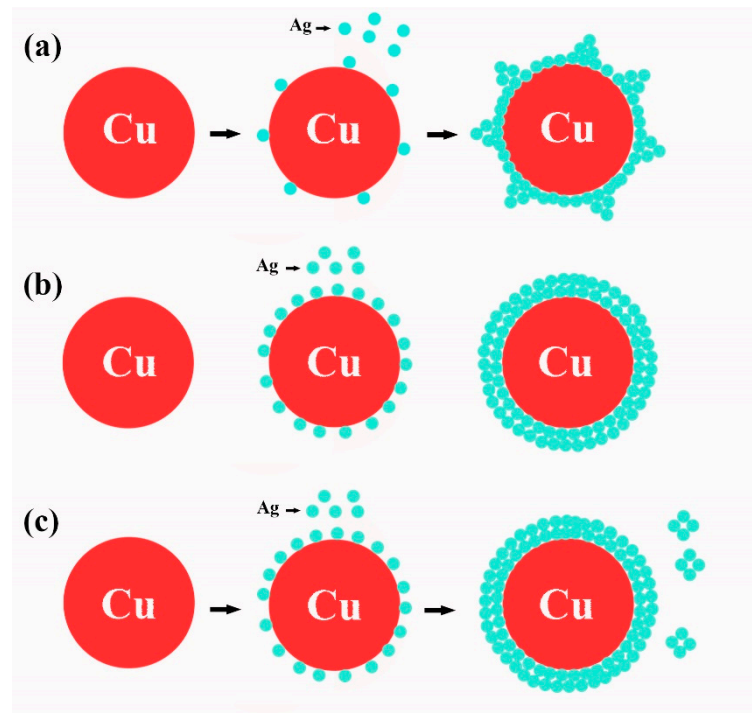


Figure 9. Silver plating model with different main salt addition rates: (a) 3–5 mL/min, (b) 8–10 mL/min, and (c) 13–15 mL/min.

The reaction of ascorbic acid reducing silver ions is as follows:



The electrode reaction of ascorbic acid is as follows:



Among them, the standard electrode potential of $\text{C}_6\text{H}_6\text{O}_6/\text{C}_6\text{H}_8\text{O}_6$ is $\varphi^\ominus = 0.08 \text{ V}$. Based on the Nernst equation, the relationship between the electrode potential of $\text{C}_6\text{H}_6\text{O}_6/\text{C}_6\text{H}_8\text{O}_6$ and pH is [27,28] as follows:

$$\varphi = \varphi^\ominus - \frac{0.0591}{n} \lg \frac{c(\text{C}_6\text{H}_8\text{O}_6)}{c(\text{C}_6\text{H}_6\text{O}_6)c(\text{H}^+)^2} \quad (4)$$

The reducing power of ascorbic acid is closely related to the pH of the reaction system. In an alkaline environment, ascorbic acid exhibits higher reducibility. During the chemical silver plating process, the pH of the reaction system changes as the silver amine solution is added. When the silver complex solution is added at a rate of 3–5 mL/min at the start of the reaction, the pH of the system is 8, and it changes gradually throughout the reaction. Initially, the reducibility of ascorbic acid is relatively low, which reduces the reaction rate between the reducing agent and silver complex ions. This delay in the reduction of silver leads to a lower nucleation rate on the copper powder surface, leading to the deposition of silver on the surface in the form of discrete particles. As the reaction progresses, these granular silver particles are prone to detaching from the powder surface due to collisions and other factors, leading to an increase in free silver. This process is illustrated in Figure 9a.

When the main salt addition rate is 8–10 mL/min, the silver particles deposited on the copper powder surface are small and uniform, resulting in a smooth and flat surface with the silver layer completely covering the copper core. This leads to a silver-coated copper

powder with low free silver content. During the chemical plating reaction, a relatively fast addition of the main salt solution increases the concentration of silver complex ions in the reaction system. This helps create a favorable alkaline environment for the reducing agent, enhancing the reaction rate and driving the chemical equilibrium to the right, thereby improving the conversion rate of silver ions. Since heterogeneous nucleation on the surface of the copper powder is preferred over homogeneous nucleation, a large number of silver particles initially precipitate and nucleate on the copper surface. These particles continue to accumulate, forming a continuous silver coating, which reduces the free silver content in the final silver-coated copper powder. Its growth model is shown in Figure 9b.

When the main salt is added at a rate of 13–15 mL/min, the powder contains a higher amount of free silver. This occurs because the rapid addition of the main salt causes concentrations of the reducing agent and complexing agent in the solution to rise too quickly. According to Weimarn's law, the formation of new phases during precipitation involves two key processes: nucleation and growth [29,30]. The relative rates of these two processes will determine the overall deposition of particles, where

The nucleation rate u_1 is as follows:

$$u_1 = \frac{K(c - c_s)}{c_s} \quad (5)$$

The crystal growth rate u_2 is as follows:

$$u_2 = \frac{DA(c - c_s)}{\delta} \quad (6)$$

where u_1 is the nucleation rate; K is the nucleation rate constant; c is the actual concentration of solute in the solution; c_s is the solubility of the solute; u_2 is the crystal nucleus growth rate; D is the diffusion coefficient; A is the crystal nucleus growth constant; δ is the thickness of the solid–liquid interface diffusion layer.

When the addition rate is too high, the concentration of silver complex ions in the solution becomes excessively high, causing the nucleation rate (u_1) to exceed the crystal growth rate (u_2). In this case, the rate of silver nucleus formation exceeds the growth rate of the silver nuclei on the surface of the copper powder. As a result, silver particles tend to nucleate independently in the solution rather than adhering to the copper surface. This leads to the formation of free silver, which increases the amount of uncoated silver in the final silver-coated copper powder. The growth process is depicted in Figure 9c.

3.4. Effect of Dispersant Concentration on Silver Deposition

During the preparation of silver-coated copper powder through chemical plating, polymer compounds with long-chain structures are commonly used as dispersants (or stabilizers) to prevent powder agglomeration. Representative dispersants include polyvinylpyrrolidone (PVP), polyethylene glycol (PEG), gelatin, and gum arabic. These dispersants adsorb onto the surface of the powder particles, and their long-chain molecular structure creates a steric hindrance effect, which physically prevents the powder particles from coming into close contact with one another. As a result, collisions between particles are minimized, thereby reducing the tendency for agglomeration and ensuring a more uniform dispersion of the powder during the chemical plating process.

The effect of PVP concentration on free silver in the preparation of silver-coated copper powder by chemical plating, with PVP as a dispersant, is investigated. When preparing the copper powder suspension, PVP is added at concentrations of 0 g/L, 0.5 g/L, 1.0 g/L, 1.5 g/L, and 2.0 g/L, respectively.

As shown in Figure 10, when the PVP concentration is low (less than 1.0 g/L), the silver layer particles on the surface of the copper powder become more prominent, and a small amount of free silver is formed. This is because PVP has a multi-dentate ligand structure, and through the coordination of its internal acyl groups, it can interact with Ag^+ ions, playing both a coordination and mechanical inhibition role. PVP acts as a surfactant in mainly two ways. First, its long molecular chain coats the surface of the powder particles, prevents agglomeration, and controls the growth of silver nanoparticles. Second, PVP possesses a polar vinyl polymer skeleton with N-C=O groups, which can be easily adsorbed on the surface of silver nanocrystals, lowering their growth rate [31]. By controlling the growth rate of the crystal surface, PVP affects the adsorption and desorption kinetics on different crystal planes. This selective adsorption leads to anisotropic growth of the silver nanocrystals, as PVP molecules preferentially adsorb onto specific crystal planes, lowering the growth rate of these planes compared to others. As a result, the morphology of the silver nanocrystals becomes controlled, with certain crystal planes growing slower than others. However, when the PVP concentration is too low, its ability to effectively control the growth of silver nanoparticles is limited, leading to uneven silver deposition on the copper powder surface.

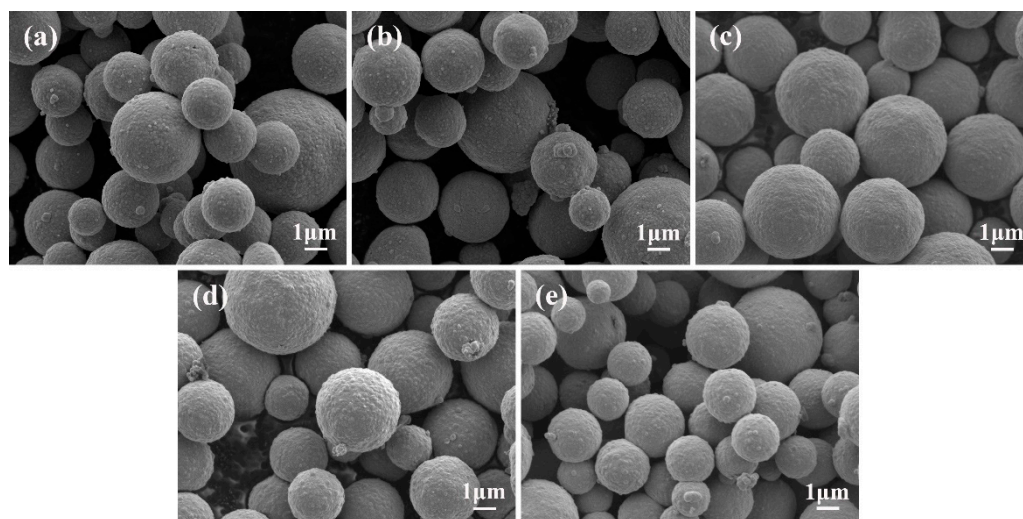


Figure 10. SEM images of silver-coated copper powders prepared with different PVP concentrations: (a) 0 g/L, (b) 0.5 g/L, (c) 1.0 g/L, (d) 1.5 g/L, and (e) 2.0 g/L.

When the PVP concentration is high (greater than 1.0 g/L), the amount of PVP adsorbed on the surface of the silver particles increases, which in turn enhances the steric hindrance on the particle surface. This increased hindrance prevents the subsequent silver atoms from effectively contacting and adhering to the surface of the silver powder particles, thereby hindering the deposition of silver onto the copper powder surface. When the PVP concentration is too high (>1.0 g/L), the concentration of PVP molecules in the solution increases, forming a thicker coating layer on the surface of the silver-coated copper powder. A too-thick PVP layer increases the difficulty of coating the silver layer, resulting in uneven silver plating, which causes an uneven surface of the silver-coated copper powder. High concentrations of PVP accumulate on the particle surface to form a relatively viscous colloid. These colloids may hinder the uniform deposition of silver, resulting in an uneven silver coating. High concentrations of PVP increase the viscosity of the solution, which affects the fluidity during the silver coating process. The high viscosity of the solution may cause uneven deposition of silver ions on the particle surface, further exacerbating the problem of an uneven silver layer. The high-viscosity solution has poor fluidity, and the diffusion rate of silver ions on the particle surface is slowed down, resulting in uneven

silver deposition area and uneven surface. The experimental results have shown that when the PVP concentration is at its optimum, i.e., 1.0 g/L, the surface of the silver-coated copper powder remains smooth, and there is no free silver. This concentration strikes a balance between adequate adsorption on the copper powder surface to prevent agglomeration, while still allowing for efficient and uniform silver deposition. As a result, the silver coating is smooth, and the quality of the prepared silver-coated copper powder is enhanced.

4. Conclusions

1. In chemical plating, there are three main reasons for the generation of free silver. The main principle of chemical plating is that silver first forms silver nuclei on the surface of copper powder and then grows on the surface of copper powder to completely cover the copper particles, that is, the reaction is divided into two parts: nucleation and growth. 1. Under certain specific conditions, the nucleation rate of silver on the surface of copper powder is low. Although the crystal nucleus can grow, the amount of silver deposited in the area with silver nuclei will increase, and silver will be attached to the surface of copper powder in the form of large particles. Since the reaction is carried out under ultrasonic and mechanical stirring conditions, the large particles of silver deposited on the surface will fall off in the collision with other powder particles. 2. When the nucleation rate of crystal nucleation is greater than the crystal growth rate, silver will nucleate and grow alone to form free silver. 3. In order to prevent powder clustering in chemical plating, dispersants are added to the reaction solution. A higher dispersant concentration will cause the dispersant molecules to form a thicker coating layer on the surface of silver-coated copper powder. Too thick a coating layer will increase the difficulty of coating the silver layer, resulting in uneven silver plating and thus generating free silver.
2. Strength of complexing ability of the complexing agent with silver will affect the stability of the plating solution. A complexing agent with strong complexing ability with silver ions will increase stability of the plating solution, provide better control of the reaction rate, and reduce free silver content in the powder.
3. Temperature affects the growth and grain size of silver. When the temperature is low, the silver particles deposited on the surface of the copper powder are larger and will detach during the subsequent stirring and collision and exist in a free form.
4. The main salt addition rate affects the pH value of the reaction system and the nucleation and growth of silver on the copper powder surface. When this rate is 8–10 mL/min, it can provide a good alkaline environment for the reducing agent, thereby increasing the reaction rate and the conversion rate of silver ions. This is conducive to the formation of a continuous and uniform coating and reduces the free silver content in the prepared silver-coated copper powder.
5. When the concentration of PVP is high, a mucous film is formed on the surface of the copper powder, which hinders contact between the silver powder particles on the surface of the copper powder and the silver complex ions, affecting the deposition of silver on the surface of the copper powder, resulting in an increase in free silver content in the prepared powder. When the PVP concentration is 1.0 g/L, the surface of the prepared silver-coated copper powder is smooth and there is no free silver.

Author Contributions: Data curation, J.C.; formal analysis, J.C.; supervision, X.Z. and X.L.; investigation, J.C., X.Z., N.Y. and B.Y.; writing original draft, J.C. All authors have read and agreed to the published version of the manuscript.

Funding: This research received no external funding.

Institutional Review Board Statement: Not applicable.

Informed Consent Statement: Not applicable.

Data Availability Statement: Data are contained within the article.

Conflicts of Interest: Author Xiang Li was employed by the company Yunnan Spring New Material Co., Ltd. The remaining authors declare that the research was conducted in the absence of any commercial or financial relationships that could be construed as a potential conflict of interest.

References

1. Jun, H.Y.; Lee, E.J.; Ryu, S.O. Synthesis and characterization of copper ink and direct printing of copper patterns by inkjet printing for electronic devices. *Curr. Appl. Phys.* **2020**, *20*, 853–861. [[CrossRef](#)]
2. Zhu, Y.; Hu, Y.G.; Zhu, P.L.; Zhao, T.; Liang, X.W.; Sun, R.; Wong, C.P. Enhanced oxidation resistance and electrical conductivity copper nanowires-graphene hybrid films for flexible strain sensors. *New J. Chem.* **2017**, *41*, 4950–4958. [[CrossRef](#)]
3. Jeong, G.; Jung, S.; Choi, Y.; Lee, J.; Seo, J.; Kim, D.S.; Park, H. A highly robust and stable graphene-encapsulated Cu-grid hybrid transparent electrode demonstrating superior performance in organic solar cells. *J. Mater. Chem. A* **2018**, *6*, 24805–24813. [[CrossRef](#)]
4. Zhang, X.M.; Yang, X.L.; Wang, B. Fabrication of silver plated copper powders to apply in flexible conductive films for strain sensor. *J. Mater. Sci.-Mater. Electron.* **2022**, *33*, 8096–8103. [[CrossRef](#)]
5. van Impelen, D.; González-García, L.; Kraus, T. Low-temperature sintering of Cu@Ag microparticles in air for recyclable printed electronics. *J. Mater. Chem. C* **2024**, *12*, 12882–12889. [[CrossRef](#)]
6. Yuan, X.H.; Liang, S.Z.; Ke, H.Z.; Wei, Q.F.; Huang, Z.J.; Chen, D.S. Photocatalytic property of polyester fabrics coated with Ag/TiO₂ composite films by magnetron sputtering. *Vacuum* **2020**, *172*, 8. [[CrossRef](#)]
7. Gao, D.G.; Liu, J.J.; Lyu, L.H.; Li, Y.J.; Ma, J.Z.; Baig, W. Construct the Multifunction of Cotton Fabric by Synergism between Nano ZnO and Ag. *Fiber. Polym.* **2020**, *21*, 505–512. [[CrossRef](#)]
8. Zhang, X.M.; Yang, X.L.; Wang, B. Electrical properties of electrically conductive adhesives from epoxy and silver-coated copper powders after sintering and thermal aging. *Int. J. Adhes. Adhes.* **2021**, *105*, 7. [[CrossRef](#)]
9. Titkov, A.I.; Logutenko, O.A.; Vorob'yov, A.M.; Gerasimov, E.Y.; Bulina, N.V.; Yukhin, Y.M.; Lyakhov, N.Z. Synthesis of Cu@Ag Nanoparticles with a Core-Shell Structure Stabilized with Oxyethylated Carboxylic Acid. *Russ. J. Gen. Chem.* **2019**, *89*, 100–105. [[CrossRef](#)]
10. Sun, Z.; Cheng, N.; Chen, F.; Lou, X.L.; Tong, X.Y.; Zhao, J.W.; Zhang, H.W. Preparation of micron-scale Cu@Ag conductive particles by displacement coating to reinforce epoxy conductive adhesives. *New J. Chem.* **2021**, *45*, 10089–10097. [[CrossRef](#)]
11. Lee, S.; Wern, C.; Yi, S. Novel Fabrication of Silver-Coated Copper Nanowires with Organic Compound Solution. *Materials* **2022**, *15*, 16. [[CrossRef](#)]
12. Varol, T.; Güler, O.; Akçay, S.B.; Aksa, H.C. Novel advanced copper-silver materials produced from recycled dendritic copper powders using electroless coating and hot pressing. *Powder Metall.* **2022**, *65*, 390–402. [[CrossRef](#)]
13. Verma, A.; Pal, S.; Kuntail, J.; Kamal, N.; Mandal, R.K.; Sinha, I. Visible light enhanced *p*-nitrophenol reduction by glycerol over Ag/Cu core-shell bimetallic nanocatalysts. *J. Environ. Chem. Eng.* **2021**, *9*, 10. [[CrossRef](#)]
14. Sabira, S.F.; Kasabe, A.M.; Mane, P.C.; Chaudhari, R.D.; Adhyapak, P.V. Selective antifungal and antibacterial activities of Ag-Cu and Cu-Ag core-shell nanostructures synthesized in-situ PVA. *Nanotechnology* **2020**, *31*, 13. [[CrossRef](#)] [[PubMed](#)]
15. Ortega, E.V.; Berk, D. Precipitation of silver powders in the presence of ethylenediamine tetraacetic acid. *Ind. Eng. Chem. Res.* **2006**, *45*, 1863–1868. [[CrossRef](#)]
16. Sun, H.P.; Wang, K.J.; Cai, X.L.; Yue, G.; Chen, Y.G. Preparation and Performance of Silver Coated Copper Powder. In Proceedings of the 3rd International Conference on Advanced Engineering Materials and Technology (AEMT 2013), Zhangjiajie, China, 11–12 May 2013; Trans Tech Publications Ltd.: Zhangjiajie, China, 2013; pp. 1057–1062.
17. Koczur, K.M.; Mourdikoudis, S.; Polavarapu, L.; Skrabalak, S.E. Polyvinylpyrrolidone (PVP) in nanoparticle synthesis. *Dalton Trans.* **2015**, *44*, 17883–17905. [[CrossRef](#)]
18. Cholan, S.; Shanmugam, N.; Kannadasan, N.; Sathishkumar, K.; Deivam, K. Effect of poly ethylene glycol (PEG) as surfactant on cerium doped ZnS nanoparticles. *J. Mater. Res. Technol.-JMRT* **2014**, *3*, 222–227. [[CrossRef](#)]
19. Yang, G.N.; Zou, Q.Y.; Wang, P.Y.; Lai, H.Q.; Lai, T.; Zeng, X.; Li, Z.; Luo, J.Y.; Zhang, Y.; Cui, C.Q. Towards understanding the facile synthesis of well-covered Cu-Ag core-shell nanoparticles from a complexing model. *J. Alloys Compd.* **2021**, *874*, 10. [[CrossRef](#)]
20. Jasni, A.B.; Yoshihara, S. Electrodeposition of Silver in Cyanide-Free Solution Containing Pyrimidine Derivative as a Complexing Agent. *J. Electrochem. Soc.* **2023**, *170*, 10. [[CrossRef](#)]
21. Liu, A.M.; Ren, X.F.; Zhang, J.; Li, D.Y.; An, M.Z. Complexing agent study for environmentally friendly silver electrodeposition(II): Electrochemical behavior of silver complex. *RSC Adv.* **2016**, *6*, 7348–7355. [[CrossRef](#)]

22. Christophe, J.; Guilbert, G.; Rayée, Q.; Poelman, M.; Olivier, M.G.; Buess-Herman, C. Cyanide-Free Silver Electrochemical Deposition on Copper and Nickel. *J. Electrochem. Soc.* **2018**, *165*, D676–D680. [[CrossRef](#)]
23. Huang, Y.; Wu, F.S.; Zhou, Z.; Zhou, L.Z.; Liu, H. Fabrication of fully covered Cu-Ag core-shell nanoparticles by compound method and anti-oxidation performance. *Nanotechnology* **2020**, *31*, 9. [[CrossRef](#)]
24. Purdy, S.C.; Muscat, A.J. Coating nonfunctionalized silica spheres with a high density of discrete silver nanoparticles. *J. Nanopart. Res.* **2016**, *18*, 10. [[CrossRef](#)]
25. Jundale, R.B.; Bari, A.H.; Kulkarni, A.A. Insights into the Synthesis and Kinetics of Silver-on-Silica Core-Shell Particles. *Langmuir* **2023**, *39*, 9681–9692. [[CrossRef](#)] [[PubMed](#)]
26. Durante, O.; Granata, V.; Fittipaldi, R.; Neilson, J.; Carapella, G.; Chiadini, F.; DeSalvo, R.; De Simone, R.; Dinelli, F.; Fiumara, V.; et al. Role of oxygen vacancies in the structural phase transformations of granular TiO₂ thin films. *Surf. Interfaces* **2023**, *37*, 11. [[CrossRef](#)]
27. Stojanov, L.; Mirceski, V. A Theoretical and Experimental Square-Wave Voltammetric Study of Ascorbic Acid in Light of Multi-Step Electron Transfer Mechanism. *J. Electrochem. Soc.* **2023**, *170*, 10. [[CrossRef](#)]
28. Niu, S.Q.; Li, S.W.; Du, Y.C.; Han, X.J.; Xu, P. How to Reliably Report the Overpotential of an Electrocatalyst. *ACS Energy Lett.* **2020**, *5*, 1083–1087. [[CrossRef](#)]
29. Chen, X.; Huang, K.; Wang, C.Y. Facile synthesis of monodispersed copper oxalate flaky particles in the presence of EDTA. *Int. J. Miner. Metall. Mater.* **2018**, *25*, 762–769. [[CrossRef](#)]
30. Rawlings, J.B.; Miller, S.M.; Witkowski, W.R. Model identification and control of solution crystallization processes: A review. *Ind. Eng. Chem. Res.* **1993**, *32*, 1275–1296. [[CrossRef](#)]
31. Gils, P.S.; Ray, D.; Sahoo, P.K. Designing of silver nanoparticles in gum arabic based semi-IPN hydrogel. *Int. J. Biol. Macromol.* **2010**, *46*, 237–244. [[CrossRef](#)]

Disclaimer/Publisher's Note: The statements, opinions and data contained in all publications are solely those of the individual author(s) and contributor(s) and not of MDPI and/or the editor(s). MDPI and/or the editor(s) disclaim responsibility for any injury to people or property resulting from any ideas, methods, instructions or products referred to in the content.